Journal of Computational Design and Engineering 6 (2019) 260–268

Contents lists available at ScienceDirect

Journal of Computational Design and Engineering

journal homepage: www.elsevier.com/locate/jcde

Fail-safe optimization of beam structures

Julian Kajo Lüdeker *, Benedikt Kriegesmann

Hamburg University of Technology, Am Schwarzenberg-Campus 4, 21073 Hamburg, Germany

ARTICLE INFO

Article history:
Received 27 August 2018
Received in revised form 12 January 2019
Accepted 21 January 2019
Available online 23 January 2019

Keywords:
Fail-safe
Lattice structures
Optimization
Stress constraints

ABSTRACT

In the current work, a fail-safe optimization of beam structures is carried out. This approach may provide an insight into the robustness of lattice structures. The use of beam elements allows a commonly used engineering approach for obtaining a fail-safe design to be applied. This consists of removing one beam element at a time and optimizing the remaining structure. At the end of the process, the maximum beam radii are used for the final design. This approach is computationally extremely expensive for lattice structures, as it requires one optimization per removed beam. In our contribution, we show that the design obtained from this approach does not actually achieve the desired fail-safe behaviour. We therefore apply a multi-model approach in which the fail-safe requirement is an optimization constraint. This is still computationally demanding and therefore, methods for reducing the number of failure cases to be considered within the optimization are discussed. Furthermore, the *p*-norm is applied to the stress constraints to reduce the computational effort for the gradient calculation. Reduction of failure cases and use of the *p*-norm have opposite effects on the conservatism of the result and therefore compensate each other to some extent.

1. Introduction

The advances in additive layer manufacturing have affected not only the application of topologically optimized structures but also the use of lattice structures. By lattice structures, we mean structures that consist of a very large number of beam-like members, often constructed from a repeated unit cell. Compared to solid structures, lattice structures show better noise and crash absorption characteristics, and they are expected to be have a better fail-safe behaviour. For certain airframe structures the certification specifications for large aeroplanes, CS-25 (Certification Specifications for Large Aeroplanes, 2012) require the design of a "multiple load path construction" and also require that "the aeroplane may function safely with an element missing". In other words, these structures need to be fail-safe by being able to resist the design load even if one load path fails. Lattice structures typically have many more load paths than solid structures, and therefore they are assumed to be closer to fail-safe than solid structures. However, optimizing lattice structures without requiring them to be fail-safe in the optimization cannot lead to a fail-safe design. If an optimized design was fail-safe, it would not be an optimum of the original optimization problem.

Topology optimization methods are typical methods for computer aided design of lightweight structures. Interpolation schemes in material penalization approaches (SIMP, RAMP) (Sigmund & Maute, 2013) for topology optimization are physically motivated, hence it is possible to find unit cells for a given volume fraction (equal to the design variable) that represent the mechanical material properties in the same way as the interpolation scheme (Sigmund, 2000). The design of unit cells with a given set of mechanical properties can also be achieved with material penalization methods, (e.g. geometrical nonlinearities (Wang, Sigmund, & Jensen, 2014) or stress constraints (Collet, Noël, Bruggi, & Duysinx, 2018)). In practice, additively manufactured lightweight structures are often filled up using a predefined lattice unit cell, without considering any kind of interpolation scheme. These bone-like structures are not necessarily optimal in terms of mechanical properties (Sigmund, 1999), but they appear to fulfil the fail-safe conditions. This statement must be investigated, since structural failure is mainly driven by the maximum stress. Due to stress concentrations at the lattice connections and a much lower volume fraction, the maximum stresses appearing in lattice structures are clearly higher than in full material structures and the pertinence of each member may be even more important, due to the high interdependencies that affect the overall load capacity. This kind of lattice structure can be modelled with beam elements,

Peer review under responsibility of Society for Computational Design and Engineering.

* Corresponding author.
E-mail addresses: julian.luedeker@tuhh.de (J.K. Lüdeker), benedikt.kriegesmann@tuhh.de (B. Kriegesmann).

https://doi.org/10.1016/j.jcde.2019.01.004
2288-4300/

making it easier to formulate a fail-safe requirement. Each beam element is interpreted as a load path. If one element fails, the remaining structure must be able to carry the load without exceeding a maximum allowed stress level.

Considerations of fail-safe design during the optimization of truss structures have already been addressed by Sun et al. in 1976 (Sun, Arora, & Haug, 1976). These authors applied stress, buckling and displacement constraints for each failure case. Due to the large number of constraints and the computational limits, this approach is restricted to relatively small examples. For bigger models, Sun et al. only consider a few failure cases at a time. Initial ideas for considering fail-safe requirements in topology optimization using solid isotropic material penalization (SIMP) are presented in Jansen, Lombaert, Schevenels, and Sigmund (2013) and implemented in commercial software (Zhou & Fleury, 2016). Instead of applying the fail-safe conditions as additional constraints of the optimization problem, as in Sun et al. (1976), the objective function is formulated as the maximum compliance of all subproblems, where each subproblem represents a failure case. This formulation results in more robust designs, but it does not guarantee that the resulting structure is fail-safe in terms of the allowed stress. Considering stress constraints within the SIMP formulation, (e.g. as suggested in Duysinx & Bendsøe (1998) could be a way of incorporating the fail-safe requirement, but this would further increase the computational costs, which are already very demanding for this fail-safe approach.

It should be emphasized that the fail-safe requirement considered in this paper does not include the progressive failure due to overloading. Therefore, the current work differs from studies on analysis and optimization redundancy, e.g., (Grimmelt & Schuëller, 1982; Murotsu, Shao, & Watanabe, 1994), where the structure fails progressively by failure of each member or joint. Similarly, the fail-safe optimization of bolt patterns given in Serafinska, Özenç, and Kaliske (2017) considers crack propagation.

As highlighted by Zhou and Fleury (2016), fail-safe optimization should not be confused with reliability-based or robust design optimization (see, e.g., Schuëller & Valdebenito, 2010). Both approaches may lead to similar results, but the underlying concepts are very different. Robust design optimization requires the embedding of a probabilistic analysis. Fail-safe design optimization requires the definition of failure cases and corresponding constraints. It seems reasonable to combine these different concepts (Cid Bengoa, Baldomir, Hernández, & Romera, 2018), in order to provide more robust fail-safe designs.

In the current study, mass minimization of lattice structures subject to stress constraints is carried out, where the lattice is modelled with beam elements. An engineering approach which is often used in practice is applied, to obtain a fail-safe structure. This approach is not only computationally demanding, but also fails to lead to the desired results. Therefore, a rigorous formulation of the optimization with fail-safe requirements is used, and various possibilities for reducing the computational effort are discussed. For beam structures it is much simpler to consider stress constraints in the optimization than, for instance in topology optimization. The authors ultimately draw conclusions that are also valid for stress-constrained fail-safe optimizations in general.

2. Optimization of lattice structures with stress constraints

Consider the problem of finding the design with a minimum weight for which the an allowable stress σ_{ref} is not exceeded. Given a finite element model of a lattice structure of n beam elements $e = 1 \dots n$, with circular cross sections defined by different radii r_e, the sizing optimization problem is formulated by Eq. (1).

$$\begin{aligned} &\min_{\boldsymbol{r}} V(\boldsymbol{r}) = \pi[\mathrm{diag}(\boldsymbol{r})\boldsymbol{r}]^T \boldsymbol{l} \\ &\text{subject to} \\ &c_j(\boldsymbol{r}) = \pm\sigma_i(\boldsymbol{r}) - \sigma_{ref} \leqslant 0 \quad j = 1 \dots n_c \\ &\qquad\qquad\qquad\qquad\quad i = 1 \dots n_\sigma \\ &r_{\min} \leqslant r_e \leqslant r_{\max} \qquad\qquad e = 1 \dots n \end{aligned} \tag{1}$$

Here, $\boldsymbol{r}$, $\boldsymbol{l} \in \mathbb{R}^n$ are the vectors of beam radii and constant beam lengths, where the vector of beam radii is the design vector. The stresses $\sigma_i(\boldsymbol{r})$ are compared to the allowable stress σ_{ref} at n_σ stress evaluation points. Since the stresses are bounded for positive as well as for negative values, the number of constraints is $n_c = 2n_\sigma$. This can be reduced to $n_c = n_\sigma$ by limiting the square of the stress value instead of limiting both the positive and negative values.

$$\begin{aligned} &\min_{\boldsymbol{r}} V(\boldsymbol{r}) \\ &\text{s.t.} \\ &c_i(\boldsymbol{r}) = \sigma_i(\boldsymbol{r})^2 - \sigma_{ref}^2 \leqslant 0 \quad i = 1 \dots n_\sigma \\ &r_{\min} \leqslant r_e \leqslant r_{\max} \qquad\qquad e = 1 \dots n \end{aligned} \tag{2}$$

The optimization of beam structures can lead to the same singularity problem as reported for truss structures in Kirsch (1990) and Cheng and Jiang (1992). However, in the current study, the intention is to keep the lattice-type structure and not to remove members. Therefore, none of the relaxation approaches as given in Cheng and Guo (1997) and Duysinx and Bendsøe (1998) are applied.

Using additive layer manufacturing, a huge variety of cross sections can be realized for the members. In the current paper, we focus on circular sections.

2.1. Stress measure

For detecting critical states, the stresses are evaluated at four points of a two-dimensional (Euler-Bernoulli) beam element (see Fig. 1) resulting in $n_c = n_\sigma = 4n$ constraints for the optimization problem.

The stresses in element e at the local position $\xi, \bar{y}$ (see Fig. 1) can be evaluated based on the local, nodal deformations $\boldsymbol{u}_e^{loc}$:

$$\sigma_e(\xi, \bar{y}) = E_e \boldsymbol{B}_e^T(\xi, \bar{y}) \boldsymbol{u}_e^{loc} \tag{3}$$

where E_e is the Young's modulus of the element and the vector $\boldsymbol{B}_e$ describes the relation between strain and deformations.

$$\boldsymbol{B}_e(\xi, \bar{y}) = \frac{1}{l^2} \begin{bmatrix} -l \\ 6\bar{y}(1-2\xi) \\ 2l\bar{y}(2-3\xi) \\ l \\ -6\bar{y}(1-2\xi) \\ 2l\bar{y}(1-3\xi) \end{bmatrix} \tag{4}$$

For each element e, the stresses are evaluated at the corners $\xi = 0, 1$ and $\bar{y} = -r_e, r_e$ (red points in Fig. 1):

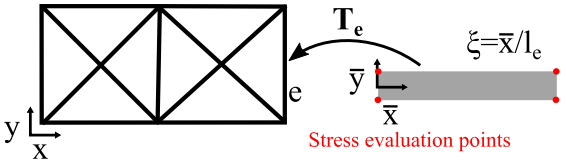

Fig. 1. Stress evaluation points on a 2D beam element.

$$\boldsymbol{\sigma}_e = \begin{bmatrix} \sigma_e(0, r_e) \\ \sigma_e(0, -r_e) \\ \sigma_e(1, r_e) \\ \sigma_e(1, -r_e) \end{bmatrix} \tag{5}$$

2.2. Sensitivity analysis

Efficient, gradient-based optimization algorithms benefit from analytical expressions for the gradients of the objective function and the constraints. The gradient of the objective function $\text{grad}V \in \mathbb{R}^n$ is given by:

$$\text{grad}(V) = \frac{\partial V}{\partial \boldsymbol{r}} = 2\pi \text{diag}(\boldsymbol{r})\boldsymbol{l} \tag{6}$$

The constraint gradient $\text{grad}(\boldsymbol{c}) \in \mathbb{R}^{n \times n_\sigma}$ requires the derivatives of the local element stresses given in Eq. (3):

$$\frac{\partial \sigma_e(\xi, \bar{y})}{\partial r_i} = E_e \left(\frac{\partial \boldsymbol{B}_e^T(\xi, \bar{y})}{\partial r_i} \boldsymbol{u}_e^{loc} + \boldsymbol{B}_e^T(\xi, \bar{y}) \frac{\partial \boldsymbol{u}_e^{loc}}{\partial r_i} \right) \tag{7}$$

The partial derivative of the strain deformation vector $\partial \boldsymbol{B}_e / \partial r_i$ at the stress evaluation points is obtained by differentiation of Eq. (4) and is equal to zero for $i \neq e$. Since the transformation matrix $\boldsymbol{T}_e$ is invariant with respect to the variable $\boldsymbol{r}$, the derivative of the local deformation vector is given by:

$$\frac{\partial \boldsymbol{u}_e^{loc}}{\partial r_i} = \boldsymbol{T}_e \frac{\partial \boldsymbol{u}_e}{\partial r_i} \tag{8}$$

Differentiating the static FEM equation $\boldsymbol{K}\boldsymbol{u} = \boldsymbol{F}$ (Michaleris, Tortorelli, & Vidal, 1994) leads to an expression for the gradient of the global deformation vector.

$$\boldsymbol{K} \frac{\partial \boldsymbol{u}}{\partial r_i} = \left(\frac{\partial \boldsymbol{F}}{\partial r_i} - \frac{\partial \boldsymbol{K}}{\partial r_i} \boldsymbol{u} \right) \tag{9}$$

Since the external forces are invariant with respect to the element radii, the term $\partial \boldsymbol{F} / \partial r_i$ equals zero. The evaluation of this gradient is computationally demanding, even if the stiffness matrix is already factorized for the solution of $\boldsymbol{u}$.

2.3. Solving the optimization problem

Approaches for a more efficient consideration of stresses, such as the use of the p-norm or clustering of stress constraints (see, e.g., Holmberg, Torstenfelt, & Klarbring, 2013) may lead to somewhat infeasible optimal designs. However, for evaluating the fail-safe optimization approaches in subsequent sections, it is important to fulfil the stress constraints as accurately as possible. Otherwise, it would be difficult to determine whether an infeasible design is obtained because of the fail-safe approach or due to the inaccuracy caused by the use of the p-norm.

Since the optimization problems (1) and (2) are solved without further measures for efficiency improvement, the problems involve a very large number of constraints. Therefore, an interior point method (see, e.g., Nocedal & Wright, 2006) is used for solving the optimization problems in the following.

2.4. Example use case

For example, a small 2D model with $n = 54$ beam elements ($E = 21,000,\ \nu = 0.3$) is used (see Fig. 2a). The length of a unit cell is 10. The degrees of freedom on the left side are fixed, and a single load ($F = 50$) is applied on the bottom right corner. The start value of the optimization for each radius is given by $r_i = 0.5$ ($V_{start} = 350.50$). The allowable range is chosen to be $10^{-4} \leqslant r_i \leqslant 1$, so that the maximum value is not reached in this example. The maximum allowable stress is set to $\sigma_{ref} = 300$.

This basic example is solved within a few seconds. Fig. 2(b) shows the reserve factor ($RF = \sigma_{ref}/\sigma$) of the optimized, intact model. The volume is reduced to $V = 30.93$ (8.82% of the initial volume) and the structure fulfils the stress constraints. We introduce the term *minimum remaining reserve factor* (MRRF) as a measure for the redundancy of a beam member. The MRRF of element e is the minimal RF of all elements for the case where element e is deleted. In Fig. 2(c), each element of the optimal design is coloured according to the MRRF. Most of the beams (coloured red/black) are necessary, to guarantee the overall load capacity of the structure.

3. Optimization of fail-safe lattice structures

This section revisits various problem formulations, which are supposed to provide an optimized, fail-safe design.

3.1. Engineering approach

The basic idea of the engineering approach for optimal fail-safe design is to perform multiple optimizations of a lattice structure and to take the maximum values of the resulting design variables (Fig. 3). In each of optimization, one of the beam elements (one load path) is removed (Fig. 4(a)), by setting its Young's modulus to a relatively low value. Removing one element is considered as a failure case, and hence, the number of failure cases n_{FC} is equal to the number of elements n.

The optimal designs found for each failure case fulfil the constraints of the optimization problem: hence, the reserve factors are greater than one. Based on engineering judgement, one might assume that using the maximal radii obtained from optimizations of all failure cases (Fig. 4(b)) provides a design that also fulfils the requirement $RF \geqslant 1$ for all failure cases, and hence that this design is fail-safe.

$$\begin{aligned} &\tilde{\boldsymbol{r}}^{(j)} = \min_{\boldsymbol{r}} V(\boldsymbol{r}) E_j \approx 0, && j = 1 \ldots n_{FC} \\ &\text{s.t.} \\ &\quad c_i(\boldsymbol{r}) = \sigma_i(\boldsymbol{r})^2 - \sigma_{ref}^2 \leqslant 0 && i = 1 \ldots n_\sigma \\ &\quad r_{\min} \leqslant r_e \leqslant r_{\max} && e = 1 \ldots n \\ &\quad r_e = \max_j \tilde{r}_e^{(j)} \end{aligned} \tag{10}$$

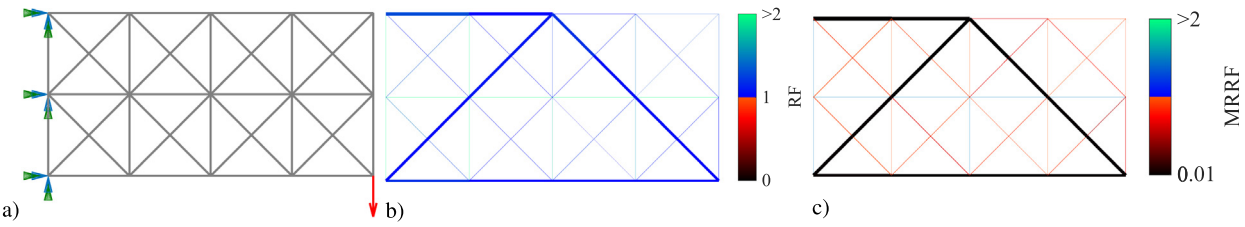

Fig. 2. Example use case: (a) boundary conditions, (b) reserve factor, (c) minimum remaining reserve factor.

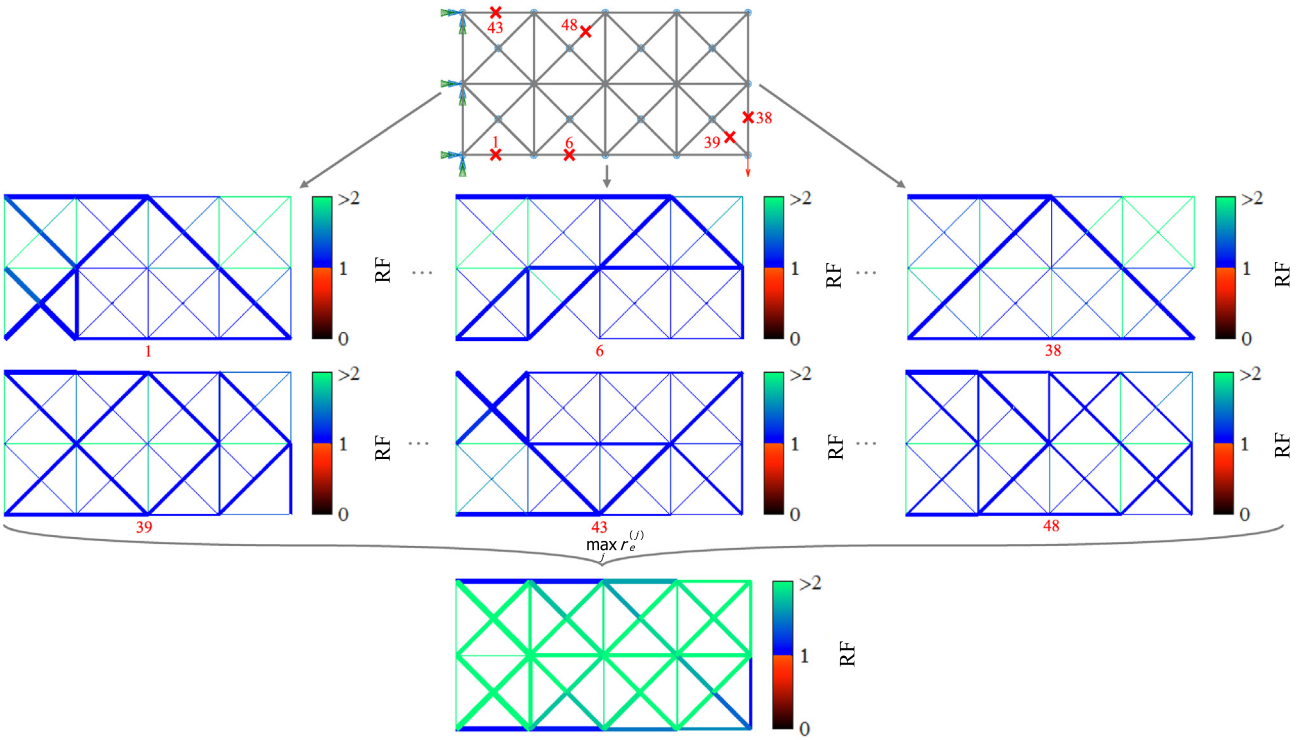

Fig. 3. Engineering approach: taking the maximum radii of all optimizations.

This approach requires n_{FC} optimizations, and the number of constraints $n_c = n_\sigma$ in each of the simulations grows linearly with the number of elements n. For the *deletion* of elements, the corresponding modulus is reduced to $E = 1$. Since every failure case is considered, $n_{FC} = n$ optimizations are performed. Each of these optimizations is limited to 100 iterations.

Fig. 4(a) shows examples of optimum designs for four failure cases. For each failure case, the stress constraints are fulfilled ($RF \geqslant 1$). When determining the fail-safe design, following the engineering approach described above and applying a failure case to that design yields the reserve factors given in Fig. 4(b).

Even though the "optimized" design considered in Fig. 4(b) has thicker members than those considered in Fig. 4(a), it does not fulfil the stress constraints for these failure cases. Obviously, taking the maximal radii heavily impacts on the load distribution within the structure. This finding is summarized by the MRRF of the "optimized" design, shown in Fig. 4(d). In contrast to the expectation, the structure obtained by the engineering approach is not conservative. It does not even fullfil the fail-safe condition.

3.2. Highly restricted approach

The requirement that a structure must be fail-safe can be formulated rigorously as part of the optimization problem, which then reads:

$$\begin{aligned} &\min_{\boldsymbol{r}} V(\boldsymbol{r}) \\ &\text{s.t.} \\ &\quad c_{ij}(\boldsymbol{r}) = \sigma_i^{(j)}(\boldsymbol{r})^2 - \sigma_{ref}^2 \leqslant 0 \quad i = 1 \dots n_\sigma \\ &\quad E_j \approx 0 \qquad\qquad\qquad\quad j = 1 \dots n_{FC} \\ &\quad r_{\min} \leqslant r_e \leqslant r_{\max} \qquad\quad e = 1 \dots n \end{aligned} \tag{11}$$

The constraint function $c_{ij}(\boldsymbol{r})$ describes the requirement that the stresses $\sigma_i^{(j)}$ may not exceed the allowed value σ_{ref} at each stress evaluation point i and for each failure case j. In contrast to the engineering approach, only one optimization, with $n_c = n_{FC} \cdot n_\sigma$ constraints, is performed, leading to a cubic growth in the constraint gradient with the number of elements (if $n_{FC} = n$). Therefore, this approach is referred to as the *highly restricted approach*. Since the constraint gradient has a high density, it cannot be stored efficiently for bigger models. Furthermore, the number of necessary FE solutions and stress evaluations per iteration is equal to the number of failure cases. Hence, the computational effort is mainly driven by the number of iterations for the optimization.

3.3. Results

Fig. 4 shows the reserve factors of the optimal designs obtained by the engineering approach (b) and the highly restricted approach (c) for four failure cases. The optimal design given by the highly restricted approach fulfils the stress constraints in each case, unlike the engineering approach. This finding is summarized in the plots of the MRRF in Fig. 4(d) and (e).

Both procedures result in qualitatively different element radii, even if the objective value (volume) is similar ($V_{eng} = 117.14$, $V_{highres} = 109.48$). In contrast to the engineering approach, the highly restricted approach is able to compensate for the failure of each single element.

4. Reducing failure cases

The highly restricted approach for fail-safe optimization requires an extremely large computational effort, due to the large number of failure cases and the corresponding gradients which require the solution of slightly different systems of equations and an adjoint system for each stress constraint of each failure case. This section discusses two approaches which aim to reduce the

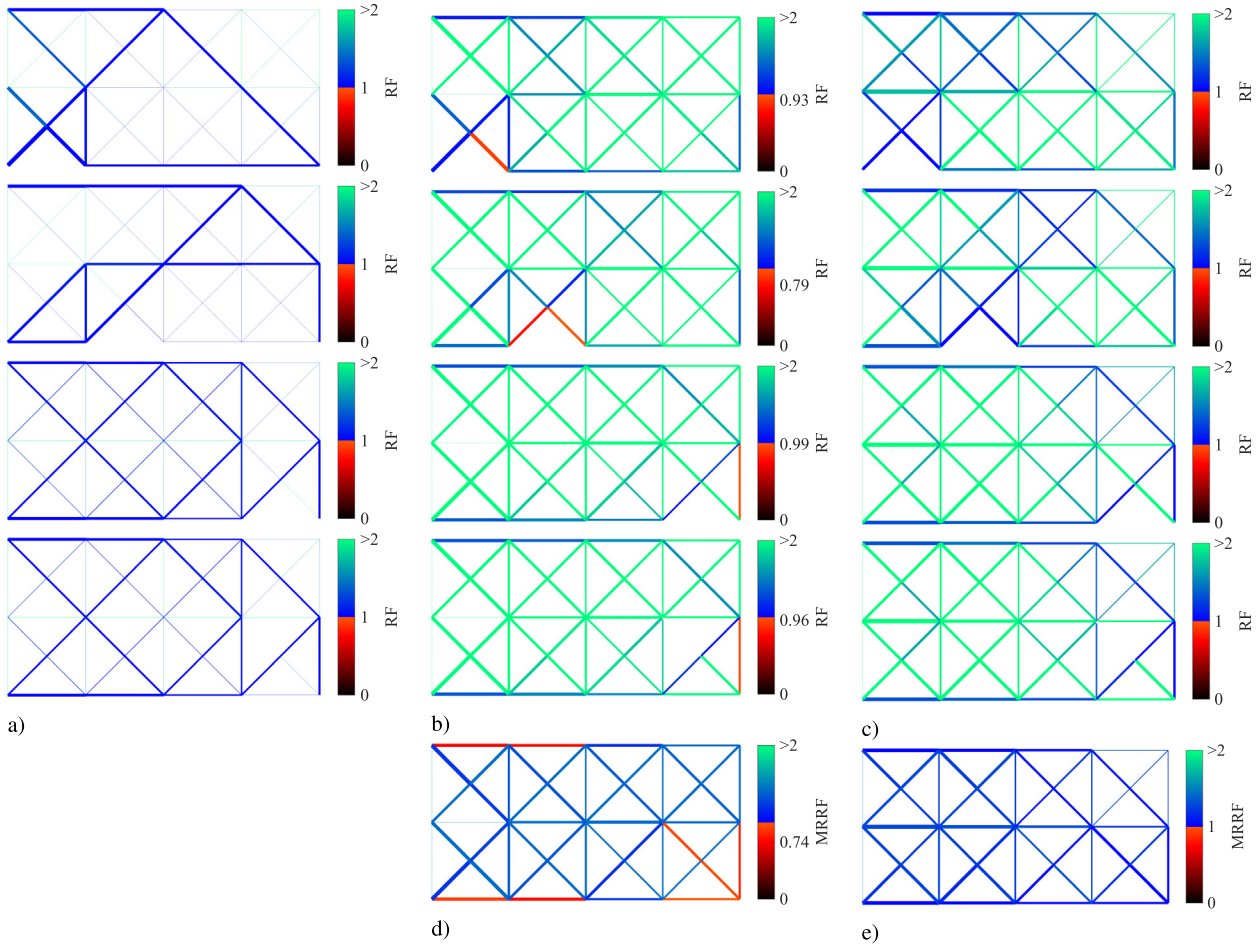

Fig. 4. (a) Exemplar results of optimizations considering a certain failure case. Reserve factors for the same failure case of the optimized structure using (b) the engineering approach and (c) the highly restricted approach and minimum remaining reserve factors (considering all failure cases) of the optimized structure using (d) the engineering approach and (e) the highly restricted approach.

number of failure cases to be considered, without losing the fail-safe capability.

One possibility is to simply neglect the failure of certain elements which are expected to play a minor role in load bearing. However, during an optimization, the radii of these elements will be increased preferentially, and hence their importance for load bearing will also change. The final result might therefore not be fail-safe.

Another approach followed subsequently is to combine two or more failure cases into one failure case. If the structure is optimized such that it fulfils stress requirements in the absence of two or more members, one might assume that it will also fulfil these requirements in the absence of only one of those members. This leads to the question of how to find the failure cases that should be combined.

In the following, two different strategies for reducing computational effort by combining failure cases are discussed. The first approach tries to combine elements which intuitively do not have a bearing function if the corresponding one fails. The second approach tries to combine failure cases based on the mechanical behaviour of the structure in its initial state. In both strategies, the failure cases to be combined are determined prior to the optimization and the combinations are not updated during the iterations. This is a very critical assumption for the second strategy, since the interdependency between different members might change rapidly during the optimization process.

4.1. Reduction based on truss model

If the lattice structure considered was a classical truss, i.e., no moments were transferred at the nodes, removing a diagonal element would cause that the connected diagonal element with the same direction to no longer attract load. Even if moments are transferred in the present structure, the elements are in fact mainly loaded via axial loads. Therefore, it is a reasonable approach to combine failure cases of elements based on the truss model as shown in Fig. 5. For a structure constructed from a given unit cell, the associated members are found simply based on geometry. A more general approach is to run all failure cases as a truss model and identify unloaded elements for each failure case.

For the example given in Section 2.4, the above given approach reduces the number of failure cases by $16/54 \approx 30\%$. This strategy does not work for all types of unit cells, as it is ultimately based on the assumption of a truss-like behaviour, which is not valid in general.

4.2. Reduction based on interdependency

In the current section, a more general reduction strategy is discussed. The basic idea is to find pairs of elements with low interdependency. To identify interdependency, we consider the change of stress in element j, if element i is removed. This is determined by calculating all failure cases. Since the objective of reducing the

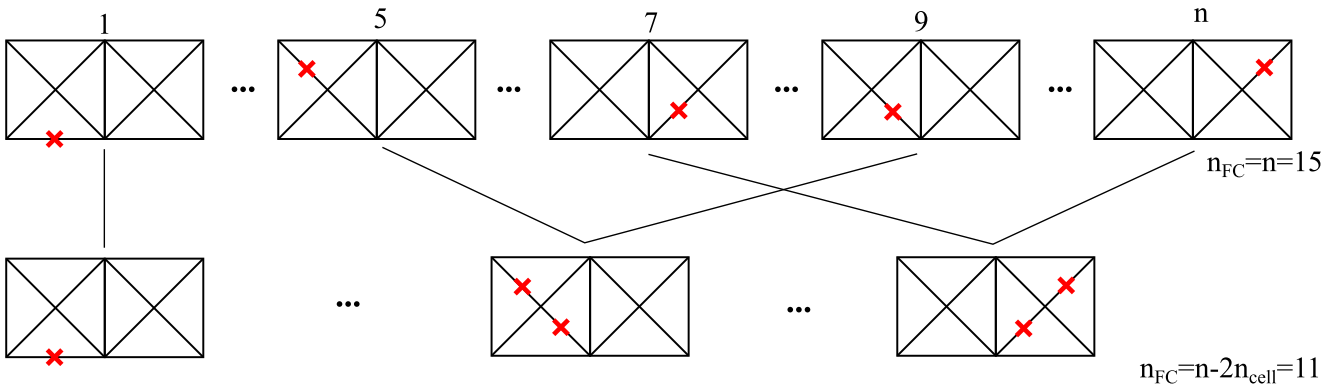

Fig. 5. Concept of reducing failure cases based on truss model.

failure cases is to avoid calculating them all, the interdependency is determined only in advance of the optimization. Due to the design updates within the optimization process, the interdependencies also change, but this fact is neglected by the current approach, as otherwise there would be no computational benefit.

For determining failure case couples, one could start with the two elements with the lowest interdependency, then continue next two elements with the lowest interdependency and so on. However, this procedure would result in couples with relatively high interdependency at the end of the selection process. Instead, a different procedure is suggested, which is outlined in the following algorithm.

Algorithm for failure case reduction based on interdependencies:

1. Determine the stresses of the initial configuration (before optimization) in intact condition and for each failure case, i.e., each beam element is removed once.
2. Determine the interdependency of all elements with each other:
   - Δ_{ij} = change of stress in element j when element i is removed.
   - The obtained matrix with interdependencies is not symmetric, but for the combined failure cases two elements will be removed at the same time. Therefore, a unique measure for the interdependency is required, which is chosen to be the maximum of both interdependencies: $\Delta_{ij}^{sym} = max(\Delta_{ij}, \Delta_{ji})$.
3. For each element i, determine the element j with the smallest interdependency $\Delta_i^{min} = min\left(\Delta_{ij}^{sym}\right)$ for $j = 1, \ldots, n$ and $j \neq i$.
4. Find the element i with the *maximal* minimal interdependency $\Delta^{maxmin} = max\left(\Delta_i^{min}\right)$ for $i = 1, \ldots, n$.
5. The element i found in 4 and the element j associated with i found in 3 are chosen as a pair for which the failure cases are considered at the same time.
6. Remove elements i and j from the matrix of interdependencies and repeat, finding a pair from 3 onwards.

The procedure described above halves the number of failure cases to be considered in the optimization.

4.3. Results

The strategies for reducing the number of failure cases described in the previous sections are applied to the example given in Section 2.4. Fig. 6 shows the optimized designs found by the engineering approach and the highly restricted approach, both without and with the two proposed strategies for reduction of

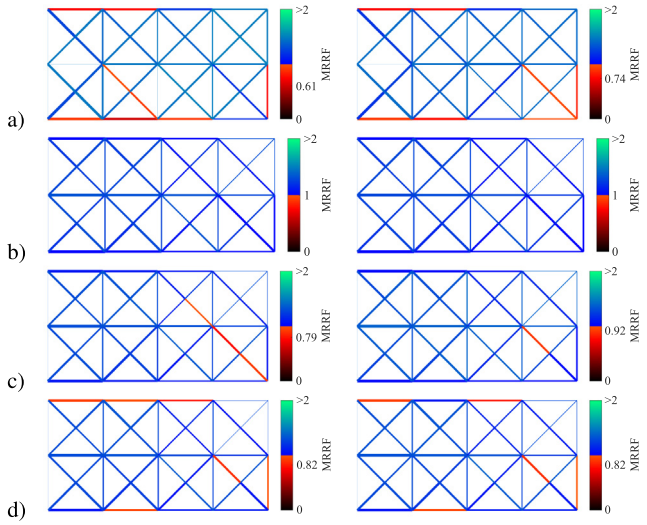

Fig. 6. Minimum remaining reserve factor (remaining eight constraints per element plus/minus, right 4 higher order constraints per element): (a) engineering approach, (b) highly restricted approach, (c) reduced failure cases based on truss model and (d) reduced failure cases based on interdependencies.

failure cases. For each approach, the results are given for eight stress constraints per element (plus/minus) as given in (1) and for four stress constraints per element (squared) as given in (2). The results are furthermore summarized in Table 1.

The optimal designs given by the highly restricted approach as well as those for the two reduction strategies are qualitatively similar. The results, however, show that the optimizations with reduced failure cases do not provide fail-safe designs. Note that the optimized designs resulting from the use of reduction strategies are feasible solutions of the corresponding problem. These solutions retain $MRRF \geqslant 1$ in the absence of two elements, but in some cases if only one of these elements is removed the *MRRF* is smaller than one. This is obviously induced by the load distribution caused by the optimization with respect to the given problem.

This finding means that neither approach presented in the previous sections for reducing the numerical effort are not conservative. Nevertheless, they provide better results than the engineering approach at lower computational cost.

An MRRF of around 0.8 where it should be 1.0 is, of course, a significant deviation from the fail-safe condition. However, one root cause of this large discrepancy is the model size. The larger the model, i.e., the more elements built into the structure, the more easily the structure will be able to compensate for the failure of one member. To demonstrate this, a larger model needs to be

Table 1
Comparison of different approaches for fail-safe design optimization.

Approach (eight constraints per element plus/minus)	Iterations	Volume fraction	MRRF	Gradient size (MB)
Without fail-safe constraint	34	8.53%	0.01	0.19
Engineering approach	–	33.38%	0.74	0.19
Highly restricted approach	28	31.23%	1	10.07
Highly restricted, reduced failure cases (truss model)	25	31.68%	0.92	5.97
Highly restricted, reduced failure cases (interdependencies)	28	30.76%	0.82	5.22
Approach (four higher order constraints per element)				
Without fail-safe constraint	29	8.82%	0.02	0.09
Engineering approach	–	33.76%	0.61	0.09
Highly restricted approach	27	31.53%	1	5.04
Highly restricted, reduced failure cases (truss model)	52	30.93%	0.79	2.99
Highly restricted, reduced failure cases (interdependencies)	100	30.61%	0.82	2.61

considered. This is however difficult to demonstrate using the highly restricted approach, since the required memory becomes too large to be handled as soon as the model becomes slightly bigger. Therefore, the use of the p-norm for the fail-safe optimization is introduced in the next section.

5. Stress constraints using p-norm

Instead of formulating the stress constraints for each stress evaluation point, the maximum stress of a failure case can be considered. The optimization problem then reads:

$$\begin{aligned} &\min_{\boldsymbol{r}} V(\boldsymbol{r}) \\ &\text{s.t.} \\ &c_j(\boldsymbol{r}) = \max_i \left[\sigma_i^{(j)}(\boldsymbol{r})\right] - \sigma_{ref} \leqslant 0 \quad i = 1 \dots n_\sigma \\ &E_j \approx 0 \qquad\qquad\qquad\qquad j = 1 \dots n_{FC} \\ &r_{\min} \leqslant r_e \leqslant r_{\max} \qquad\qquad e = 1 \dots n \end{aligned} \tag{12}$$

Since the maximum function is not differentiable, a commonly used approach for considering stresses in optimizations is to use the p-norm of all (Duysinx & Sigmund, 1998; Le, Norato, Bruns, Ha, & Tortorelli, 2009) or a certain set of stress constraints (Holmberg et al., 2013). The p-norm of a constraint vector $\boldsymbol{c}$ is given by:

$$c^{PN} = \left(\sum_{i=1}^{n_c} c_i^p\right)^{\frac{1}{p}} \leqslant \max \boldsymbol{c} \tag{13}$$

This expression converges to the maximum value in $\boldsymbol{c}$ when $p \to \infty$ and allows the use of gradient-based methods, since it is differentiable. The choice of p is critical for the optimization process (Zhou & Sigmund, 2017). Low values are too conservative, especially when there are large distinctions in the entries of $\boldsymbol{c}$. Values which are to high lead to highly non-convex restrictions of the design domain, so that the optimization algorithm is more likely to result in less-optimal local solutions. Therefore p is often heuristically increased during the optimization process.

Applying the p-norm to the stress constraint in Eq. (12) leads to:

$$c_j = \left(\sum_{i=1}^{n_\sigma} \sigma_i^{2p}\right)^{\frac{1}{p}} - \sigma_{ref}^2 \tag{14}$$

The derivative of the this constraint with respect to the stresses is given by:

$$\frac{\partial c_j}{\partial \sigma_i} = \underbrace{2\left(\sum_{k=1}^{n_\sigma} \sigma_k^{2p}\right)^{\frac{1}{p}-1}}_{C_\sigma} \sigma_i^{2p-1} \tag{15}$$

The sensitivity with respect to the design variable r_e is obtained by making use of Eqs. (7) and (9).

$$\begin{aligned} \frac{\partial c_j}{\partial r_e} &= \sum_{i=1}^{n_\sigma} \frac{\partial c_j}{\partial \sigma_i} \frac{\partial \sigma_i}{\partial r_e} \\ &= C_\sigma \sum_{i=1}^{n_\sigma} \sigma_i^{2p-1} E_i \left(\frac{\partial \overline{\boldsymbol{B}}_i^T}{\partial r_e}\boldsymbol{u} + \overline{\boldsymbol{B}}_i^T \frac{\partial \boldsymbol{u}}{\partial r_e}\right) \\ &= C_\sigma \sum_{i=1}^{n_\sigma} \sigma_i^{2p-1} E_i \left(\frac{\partial \overline{\boldsymbol{B}}_i^T}{\partial r_e}\boldsymbol{u} - \overline{\boldsymbol{B}}_i^T \boldsymbol{K}^{-1} \frac{\partial \boldsymbol{K}}{\partial r_e}\boldsymbol{u}\right) \\ &= C_\sigma \sum_{i=1}^{n_\sigma} \sigma_i^{2p-1} E_i \frac{\partial \overline{\boldsymbol{B}}_i^T}{\partial r_e}\boldsymbol{u} \\ &\quad \underbrace{-\left(\boldsymbol{K}^{-1}\left(C_\sigma \sum_{i=1}^{n_\sigma} \sigma_i^{2p-1} E_i \overline{\boldsymbol{B}}_i\right)\right)^T}_{\boldsymbol{\lambda}^T} \frac{\partial \boldsymbol{K}}{\partial r_e}\boldsymbol{u} \end{aligned} \tag{16}$$

The global B-vector $\overline{\boldsymbol{B}}_i$ is equal to the product of $\boldsymbol{T}_i \boldsymbol{B}_i$ (transformation matrix and local B-vector) sorted into the correct positions based on the indices of the corresponding degrees of freedom. The adjoint variable $\boldsymbol{\lambda}$ is derived from the following system, which is solved efficiently since $\boldsymbol{K}$ is already factorized for the solution of $\boldsymbol{u}$.

$$\boldsymbol{K}\boldsymbol{\lambda} = -C_\sigma \sum_{i=1}^{n_\sigma} \sigma_i^{2p-1} E_i \overline{\boldsymbol{B}}_i \tag{17}$$

In contrast to the previous problem formulations, there is only one constraint left for each failure case, and therefore the calculation time of the corresponding gradient is significantly shorter. Furthermore, the size of the equation system which has to be solved in the interior point method is significantly reduced, since the overall size of the fail-safe constraint is reduced from $n_{FC}^2 \cdot n_\sigma$ to $n_{FC} \cdot n_\sigma$.

Using the p-norm allows larger systems to be optimized as shown in Fig. 7. Just as in the smaller model, the model is clamped at the left edge and loaded at the lower right end, but it consists of 12 times six cells, leading to 450 elements and 498 degrees of freedom. For the optimization, p is initially set to 12 and increased to 24 after 100 iterations. For the approach using interdependencies (see Section 4.2), they are recalculated after 100 iterations.

Since the p-norm only provides a lower-bound estimation of the maximum stress, it is conservative, whereas the reduction of failure cases turns out to be non-conservative. The question that arises is in how far both effects compensate each other when they are combined. This question cannot be answered in general, as it depends on the value of p and the model itself. For the considered example, using the truss model-based reduction provides an MRRF lower than 1.0, even when it is combined with the p-norm (see Table 2 and Fig. 7). The combination of failure case reduction based on interdependencies and p-norm results in a conservative design with the lowest weight.

5.1. Computational effort

The computational effort for different optimization procedures cannot be compared directly, since the number of iterations per

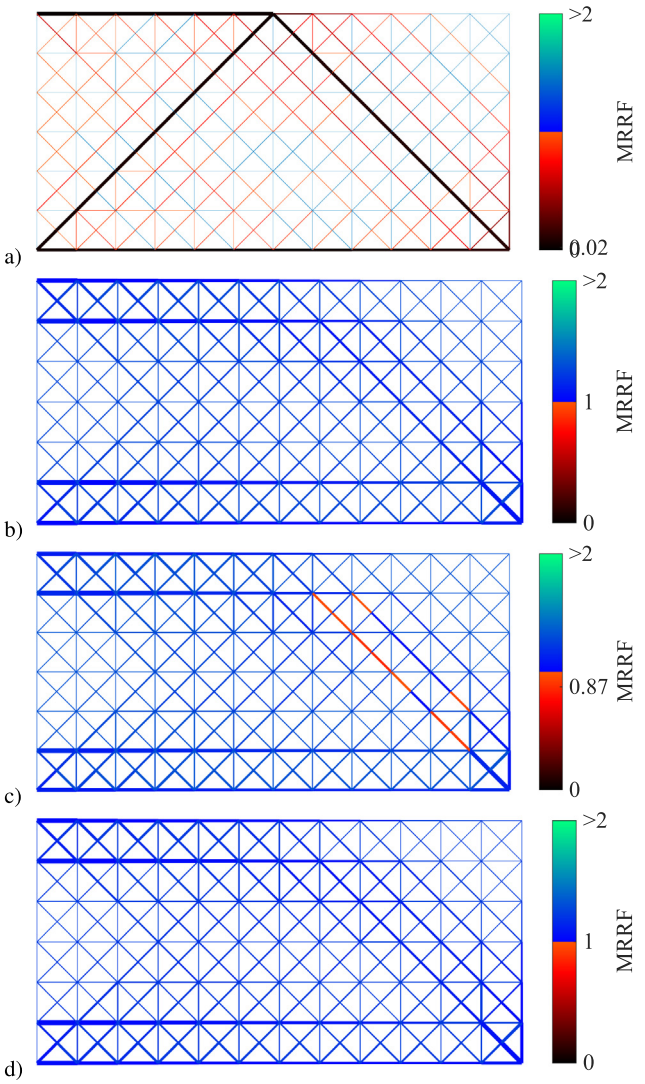

Fig. 7. Minimum remaining reserve factor for a larger model using the *p*-norm approach, considering (a) classical sizing (no *p*-norm) (b) all failure cases, (c) reduced failure cases based on truss model and (d) reduced failure cases based on interdependencies.

Table 2
Fail-safe optimization results for larger model, using *p*-norm for maximum stress estimation.

Approach	Iterations	Volume fraction	MRRF
Sizing	91	3.43%	0.02
Highly restricted approach	200	9.58%	1.06
Reduced failure cases (truss model)	200	9.32%	0.87
Reduced failure cases (interdependencies)	200	9.31%	1.04

optimization cannot be estimated a priori. Use of the engineering approach requires multiple optimizations and therefore many more iterations in total. The main issue in the highly restricted approach is the rapidly increasing growth of the constraint gradient size depending on the number of elements. This procedure is not practical, (e.g., $1e^3$ elements require 50 GB of memory storage) without using the p-norm to assemble the constraints of each failure case. Using the p-norm usually extends the number of required iterations. The only partially practical solution for fail-safe medium-sized models appears to be the highly restricted approach using the p-norm. An overview of the computational effort required for the discussed approaches is given in Table 3.

6. Conclusions and outlook

In the current work, an optimization of lattice structures is presented in which each member is modelled as an individual beam element with varying thickness. The optimization problem considered seeks to minimize the weight/volume under particular stress constraints. This set-up is used to investigate how fail-safe requirements can be embedded in the optimization. As a reference, an engineering approach for determining a fail-safe design is followed. Though this approach intuitively seems to be conservative, the designs obtained from this approach turn out not to be fail-safe. A rigorous formulation of the fail-safe optimization, in which the fail-safe requirement is considered as constraint, provides fail-safe designs. However, this procedure is computationally very demanding (which also true for the engineering approach). Therefore, possibilities for reducing the number of constraints in the optimization are investigated.

Two approaches are discussed, which reduce the number of failure cases by combining them. The optimal designs obtained from these approaches are able to sustain load in the absence of two elements, but in some cases the MRRF is below 1.0 for these structures. Therefore, the approaches with combined failure cases do not provide a fail-safe design, although the violation of this requirement is smaller than for the engineering approach.

With increasing model size, the capability of compensating for the failure of one element increases. Therefore, the violation of the fail-safe requirement becomes smaller for larger structures. However, also the need for efficiency improvement also increases and one may wish to consider even more failure cases at the same time.

When formulating the stress constraints in terms of maximum stress and approximating this using the *p*-norm, the number of constraints decreases and the adjoint method can be used for determining derivatives. This improves the efficiency, but also leads to overly conservative designs. Using the *p*-norm approach for a reduced number of failure cases allows for compensation the lack of conservatism of the failure case reduction and makes use of the efficiency improvements of both measures. However, there is no assurance that this combined approach is always conservative.

Table 3
Computational effort for the different optimization procedures depending on the number of elements n_e. Number of iterations is problem-dependent.

	Number of optimizations	Constraint gradient size	FE factorizations per iteration	Solving factorized FE LGS per iteration
Sizing	1	$n_e \times 4n_e$	1	$4n_e$
Sizing, p-Norm	1	$n_e \times 1$	1	1
Engineering approach	n_e	$n_e \times 4n_e$	1	$4n_e$
Engineering approach, p-Norm	n_e	$n_e \times 1$	1	1
Highly restricted approach	1	$n_e \times 4n_e^2$	n_e	$4n_e^2$
Highly restricted approach, p-Norm	1	$n_e \times 4n_e$	n_e	$4n_e$

The presented combination and reduction of failure cases may also be applied to topology optimization of continuous structures. Obviously, the approach presented by Jansen et al. (2013) becomes faster if two patches are removed at the same time. For the selection of such pairs of patches, the procedure presented in Section 4.2 can be used. However, also the finding that the resulting optimal structure may not be fail-safe may also apply to topologically optimized structures.

These studies emphasize that the main question in fail-safe design optimization is how to define the important failure cases, and they also show that this question cannot be answered a priori for more complex structures. Even reasoned strategies for neglecting failure cases can be critical and may not provide fail-safe designs. This complicates the reasoning for state-of-the-art fail-safe optimization, which considers only a few simple failure cases, or minimizes the maximum compliance of multiple models. Metal parts may also start to yield, so that maximum stresses may not be the critical limitation of the problem. In this case, it could be necessary to include more advanced damage criteria in the optimization, to provide a less conservative design and to fulfil fail-safe requirements at the same time.

Conflict of interest

None.

References

Certification Specifications for Large Aeroplanes (2012). Tech. Rep. CS-25, Amendment 12, European Aviation Safety Agency.

Cheng, G., & Guo, X. (1997). e-relaxed approach in structural topology optimization. *Structural Optimization, 13*, 9.

Cheng, G., & Jiang, Z. (1992). Study on topology optimization with stress constraints. *Engineering Optimization, 20*(2), 129–148 <http://www.tandfonline.com/doi/abs/10.1080/03052159208941276>.

Cid Bengoa, C., Baldomir, A., Hernández, S., & Romera, L. (2018). Multi-model reliability-based design optimization of structures considering the intact configuration and several partial collapses. *Structural and Multidisciplinary Optimization, 57*(3), 977–994. https://doi.org/10.1007/s00158-017-1789-y.

Collet, M., Noël, L., Bruggi, M., & Duysinx, P. (2018). Topology optimization for microstructural design under stress constraints. *Structural and Multidisciplinary Optimization*, 1–19. https://doi.org/10.1007/s00158-018-2045-9 <https://link.springer.com/article/10.1007/s00158-018-2045-9>.

Duysinx, P., & Sigmund, O. (1998). New developments in handling stress constraints in optimal material distribution. American Institute of Aeronautics and Astronautics Paper 98-4906, 10.

Duysinx, P., & Bendsøe, M. P. (1998). Topology optimization of continuum structures with local stress constraints. *International Journal for Numerical Methods in Engineering, 43*, 1453–1478.

Grimmelt, M. J., & Schuëller, G. I. (1982). Benchmark study on methods to determine collapse failure probabilities of redundant structures. *Structural Safety, 1*(2), 93–106. https://doi.org/10.1016/0167-4730(82)90018-2 <http://www.sciencedirect.com/science/article/pii/0167473082900182>.

Holmberg, E., Torstenfelt, B., & Klarbring, A. (2013). Stress constrained topology optimization. *Structural and Multidisciplinary Optimization, 48*, 33–47.

Jansen, M., Lombaert, G., Schevenels, M., & Sigmund, O. (2013). Topology optimization of fail-safe structures using a simplified local damage model. *Structural and Multidisciplinary Optimization, 49*(4), 657–666. https://doi.org/10.1007/s00158-013-1001-y <http://link.springer.com/article/10.1007/s00158-013-1001-y>.

Kirsch, U. (1990). On singular topologies in optimum structural design. *Structural Optimization, 2*(3), 133–142. https://doi.org/10.1007/BF01836562 <https://link.springer.com/article/10.1007/BF01836562>.

Le, C., Norato, J., Bruns, T., Ha, C., & Tortorelli, D. (2009). Stress-based topology optimization for continua. *Structural and Multidisciplinary Optimization, 41*(4), 605–620. https://doi.org/10.1007/s00158-009-0440-y <http://link.springer.com/article/10.1007/s00158-009-0440-y>.

Michaleris, P., Tortorelli, D. A., & Vidal, C. A. (1994). Tangent operators and design sensitivity formulations for transient non-linear coupled problems with applications to elastoplasticity. *International Journal for Numerical Methods in Engineering, 37*(14), 2471–2499. https://doi.org/10.1002/nme.1620371408 <http://onlinelibrary.wiley.com/doi/10.1002/nme.1620371408/abstract>.

Murotsu, Y., Shao, S., & Watanabe, A. (1994). An approach to reliability-based optimization of redundant structures. *Structural Safety, 16*(1), 133–143. https://doi.org/10.1016/0167-4730(94)00031-K <http://www.sciencedirect.com/science/article/pii/016747309400031K>.

Nocedal, J., & Wright, S. J. (2006). *Numerical optimization. Springer series in operations research and financial engineering*. New York: Springer.

Schuëller, G. I., & Valdebenito, M. (2010). Reliability-based optimization - An overview. *Computational Technology Reviews, 1*, 121–155.

Serafinska, A., Özenç, K., & Kaliske, M. (2017). A coupled approach of optimization, uncertainty analysis and configurational mechanics for a fail-safe design of structures. *International Journal for Numerical Methods in Engineering, 109*(1), 125–152. https://doi.org/10.1002/nme.5282 <http://onlinelibrary.wiley.com/doi/10.1002/nme.5282/abstract>.

Sigmund, O. (1999). On the optimality of bone microstructure. In *IUTAM symposium on synthesis in bio solid mechanics, solid mechanics and its applications* (pp. 221–234). Dordrecht: Springer.

Sigmund, O. (2000). A new class of extremal composites. *Journal of the Mechanics and Physics of Solids, 48*(2), 397–428. https://doi.org/10.1016/S0022-5096(99)00034-4 <http://www.sciencedirect.com/science/article/pii/S0022509699000344>.

Sigmund, O., & Maute, K. (2013). Topology optimization approaches. *Structural and Multidisciplinary Optimization, 48*(6), 1031–1055. https://doi.org/10.1007/s00158-013-0978-6 <http://link.springer.com/article/10.1007/s00158-013-0978-6>.

Sun, P. F., Arora, J. S., & Haug, E. J. Jr., (1976). Fail-safe optimal design of structures. *Engineering Optimization, 2*(1), 43–53. https://doi.org/10.1080/03052157608960596.

Wang, F., Sigmund, O., & Jensen, J. S. (2014). Design of materials with prescribed nonlinear properties. *Journal of the Mechanics and Physics of Solids, 69* (Supplement C), 156–174. https://doi.org/10.1016/j.jmps.2014.05.003 <http://www.sciencedirect.com/science/article/pii/S0022509614000866>.

Zhou, M., & Fleury, R. (2016). Fail-safe topology optimization. *Structural and Multidisciplinary Optimization*, 1–19. https://doi.org/10.1007/s00158-016-1507-1 <http://link.springer.com/article/10.1007/s00158-016-1507-1>.

Zhou, M., & Sigmund, O. (2017). On fully stressed design and p-norm measures in structural optimization. *Structural and Multidisciplinary Optimization, 56*(3), 731–736. https://doi.org/10.1007/s00158-017-1731-3 <https://link.springer.com/article/10.1007/s00158-017-1731-3>.